

Effects of biochar immobilization of *Serratia* sp. F4 OR414381 on bioremediation of petroleum contamination and bacterial community composition in loess soil

Xuhong Zhang^a, Manli Wu^{a,b,*}, Ting Zhang^a, Huan Gao^a, Yawen Ou^a, Mengqi Li^a

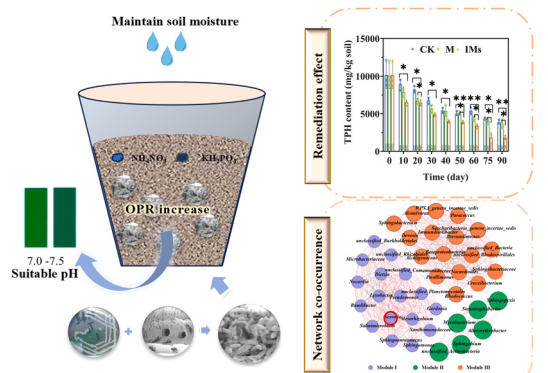
^a Key Laboratory of Environmental Engineering of Shaanxi Province, School of Environmental and Municipal Engineering, Xi'an University of Architecture and Technology, Xi'an 710055, China

^b Key Laboratory of Northwest Water Resources, Environment and Ecology, Ministry of Education, Xi'an 710055, China

HIGHLIGHTS

GRAPHICAL ABSTRACT

- Biochar immobilized strain F4 reduced soil moisture evaporation and improved soil pH.
 - Biochar application stimulated the growth of TPH degrader *Salinimicrobium sp.*
 - Biochar application upregulated *xylX*, *Am*, and *CYP450* gene expressions.
 - Nitrogen addition stimulated ammonia oxidation and denitrification.



ARTICLE INFO

Keywords:

Petroleum-contaminated soil
Biochar immobilization
Microbial community analysis
Flow cytometry
Degradation genes
Soil enzyme activity

ABSTRACT

Petroleum hydrocarbons pose a significant threat to human health and the environment. Biochar has increasingly been utilized for soil remediation. This study investigated the potential of biochar immobilization using *Serratia* sp. F4 OR414381 for the remediation of petroleum-contaminated soil through a pot experiment conducted over 90 days. The treatments in this study, denoted as IMs (maize straw biochar-immobilized *Serratia* sp. F4), degraded 82.5% of the total petroleum hydrocarbons (TPH), 59.23% of the aromatic, and 90.1% of the saturated hydrocarbon fractions in the loess soils. During remediation, the soil pH values decreased from 8.76 to 7.33, and the oxidation-reduction potential (ORP) increased from 156 to 229 mV. The treatment-maintained soil nutrients of the IMs were 138.94 mg/kg of $\text{NO}_3^- \cdot \text{N}$ and 92.47 mg/kg of available phosphorus (AP), as well as 11.29% of moisture content. The activities of soil dehydrogenase (SDHA) and catalase (CAT) respectively increased by 14% and 15 times compared to the CK treatment. Three key petroleum hydrocarbon degradation genes, including *CYP450*, *AJ025*, and *xylX* were upregulated following IMs treatment. Microbial community analysis revealed that a substantial microbial population of $1.01\text{E}+09$ cells/g soil and oil-degrading bacteria such as

* Corresponding author at: Key Laboratory of Environmental Engineering of Shaanxi Province, School of Environmental and Municipal Engineering, Xi'an University of Architecture and Technology, Xi'an 710055, China.

E-mail address: wumanli1974@hotmail.com (M. Wu).

Salinimicrobium, *Saccharibacteria genera incertae sedis*, and *Brevundimonas* were the dominant genera in IMs treatment. This suggests that the biochar immobilized on *Serratia sp.* F4 OR414381 improves soil physicochemical properties and enhances interactions among microbial populations, presenting a promising and environmentally friendly approach for the stable and efficient remediation of petroleum-contaminated loess soil.

1. Introduction

Oil pollution has emerged as a global concern, primarily because of accidental pipeline leaks during oil transportation and refinery spills [17]. Saturated hydrocarbons and aromatic hydrocarbons constitute the fundamental components of the total petroleum hydrocarbons (TPH), which are toxic, potentially lethal to humans, and resistant to rapid decomposition by soil indigenous microorganisms [10,40]. Hence, developing an effective approach for remediating petroleum-contaminated soils is imperative.

Several physicochemical, thermal, acoustic, and electrical/electromagnetic methods can be used for petroleum-contaminated soil remediation; however, most are costly and have undesirable effects [34,36]. Bioremediation is currently a promising technique, which includes the biostimulation and bioaugmentation of oil-contaminated soil [54]. Biostimulation enhances the metabolic activity of indigenous microbial communities through nutrient amendment. Nitrogen and phosphorus are essential growth-limiting nutrients for microorganisms (Shahi et al., 2016). Wu et al. (2019) demonstrated 28.3% petroleum degradation by adding exogenous N and P nutrient elements. Liu et al. [28] showed TPH removal rates of 61.59% for KNO_3 amendment and 48.55% for NH_4Cl amendment in freshly polluted soils.

Bioaugmentation includes inoculating exogenous microorganisms into contaminated soils because the native population of hydrocarbon-degrading bacteria is usually insufficient [1,53]. Previous studies have employed various species of petroleum hydrocarbon-degrading bacteria, including *Bacillus*, *Pseudomonas*, *Acinetobacter*, *Vibrio*, and *Sphingobacterium* [16,4,65]. AlKaabi et al. [4] demonstrated a 23% increase in petroleum degradation efficiency by inoculating petroleum-contaminated soil with the oil-degrading bacteria *Bacillus* and *Pseudomonas*. However, the effectiveness of bioaugmentation is dependent on context and limited by factors such as unsuitable pH, nutrient deficiency, and competition with native microorganisms, which potentially inhibit the abundance and activity of free bacteria [15,18,20–22,54].

A novel approach to addressing these challenges combines immobilized carriers with microorganisms, known as immobilized microbial technology (IMT) [9,66]. These carriers facilitate oxygen transfer, maintain the soil moisture content, and provide essential nutrients [50]. Biochar, a carbon-rich residue produced from the pyrolysis of organic matter with a large specific surface area, well-developed porous structure, and abundant functional groups, is a common immobilized carrier that enhances the bacterial adsorption capacity [3,42]. In addition, biochar stimulates the activities of enzymes such as soil dehydrogenase, polyphenol oxidase, hydrolase, and soil element cycling [21,60]. Guo et al. [16] reported that petroleum hydrocarbon removal efficiency reached 53.81% after 84 days of bioremediation using wheat bran that was biochar immobilized using three bacterial genera: *Pseudomonas*, *Acinetobacter*, and *Sphingobacterium*. Another study employed rice husk biochar and sodium alginate to immobilize fungi and achieved a diesel removal efficiency of 64.10% in highly diesel-contaminated soil after 60 days of remediation [58]. In addition, biochar-immobilized consortia were successfully applied to remediate oil refinery wastewater, demonstrating excellent operational performance with the highest removal efficiencies for chemical oxygen demand (COD) (97.9%), oil (97.4%), NH_4^+ -N (97.2%), and total nitrogen (TN) (90.2%) [48]. Building on prior research, the synergistic approach of combining biochar and bacteria TPH removal and improving contaminated soil is promising.

Although applying biochar-immobilized microorganisms has

potential for contamination remediation, the influence of biochar-immobilized microorganisms on soil physicochemical environments, functional microorganisms, and nitrogen-cycling during petroleum contamination remediation remains unclear. This study aimed to: (1) assess the remediation effects of applying biochar combined with immobilized functional microorganisms to petroleum-contaminated soil; (2) investigate the changes in soil physicochemical properties and bacterial communities during remediation; and (3) elucidate changes in soil microbial communities and functional genes during the early and late stages of remediation.

2. Materials and methods

2.1. Soil properties

Clean soil was stratified by random sampling at 0–40 cm depths from the North of Shaanxi Province, China. All soil samples were sieved through a 2 mm sieve and manually homogenized for the experiments. To prepare the petroleum-contaminated soil, 6 g of crude oil was dissolved in 250 mL of dichloromethane and added to 500 g of soil. Subsequently, the soil was thoroughly stirred every half day and air-dried in a fume hood for five days to ensure the complete evaporation of dichloromethane. Finally, the soil was aged in the dark for 21 days. The final TPH content of the soil was 10,133 mg/kg. The basic physicochemical properties of the petroleum-contaminated soils are provided in Table 1.

2.2. Biochar preparation and characteristic analysis

The maize straw was processed through a crusher to obtain small fragments (0.5–1 cm), followed by rinsing with ultrapure water, dried in an oven at 80 °C for 12 h, and collected for use. Subsequently, 200 g of dried straw fragments were placed in a 300 mL crucible and wrapped in three layers of aluminum foil to exclude air. The product was calcined in a muffle furnace (SX-5-12, Beijing Kewei Shuixing Instrument Co., Ltd, China) at 400 °C for 3 h. To obtain the biochar, the product was ground down and sieved through a 0.425 mm sieve. The biochar was immersed in a 1 mol/L HCl solution for 6 h and then rinsed with ultrapure water to obtain a pH of 6.5. The obtained biochar, labeled as J400, was dried at 80 °C for 6 h, and then stored in a sealed container. Scanning electron microscopy (SEM; Carl Zeiss Gemini SEM 360, Japan) was used to characterize the surface morphology of J400 biochar. Surface functional group information of biochar was determined using FTIR (FTIR-650S, Japan) technology. The ash content of the biochar was determined based

Table 1

Physicochemical properties of the petroleum-contaminated soil (mean ± standard deviation (SD), n = 3).

| Mean characteristics | Value |
|---|----------------------------|
| TPH (mg/kg) | 10,133 ± 210 |
| Moisture content (%) | 1.83 ± 0.23 |
| pH | 8.76 ± 0.02 |
| Oxidation-Reduction Potential (Mv) | 155 ± 2 |
| Ammonia nitrogen (mg/kg) | 1.92 ± 0.7 |
| Nitrate nitrogen (mg/kg) | 0.38 ± 0.02 |
| Available phosphorus (mg/kg) | 7.67 ± 3.22 |
| Total bacterial numbers (cells/g) | (2.30E+07) ± (9.65 E + 06) |
| Highly active bacterial numbers (cells/g) | (1.66E+07) ± (8.54E+06) |
| Catalase activity (CAT) (U/g) | 4.8 ± 0.7 |
| Soil dehydrogenase activity (SDHA) (U/g) | 4.16 ± 0.6 |

on the residue remaining after the pyrolysis. The basic properties of the biochar are shown in Fig. 1e and Table S1.

2.3. Petroleum hydrocarbon degrader *Serratia* sp. F4

Serratia sp. F4 OR414381 was isolated from the aged oil-polluted soil, sampled from an oil spill area in Changqing Oilfield, northern Shaanxi province of China ($E 108^{\circ}08'22.93''$, $N 36^{\circ}06'32.67''$). Firstly, 10 g of aged oil-polluted soil sample were put into 250 mL flask with 100 mL of phosphate-buffered saline (PBS). The solution consisted of 8.0 g of NaCl, 0.2 g of KCl, 1.44 g of Na_2HPO_4 , and 0.24 g of KH_2PO_4 dissolved in 1000 mL of sterile water with a final pH of 7.4. Thereafter, 0.5 g of crude oil (obtained from Changqing Oilfield) was added as sole carbon and energy sources under sterile conditions. Incubation was cultured at 25 °C by shaking on an oscillating incubator (180 rpm) for 7 days, 6% of the cultures were then transferred into 50 mL of PBS with 0.5 g crude oil for further enrichment. After five enrichment cycles, the petroleum hydrocarbon degrader was obtained by centrifugation (5000 rpm) for 15 min and suspended in PBS [62]. Hydrocarbon degraders were identified using high-throughput sequencing by Beijing Aoke Dingsheng Biotechnology Co. (China). The 16S rDNA gene sequence was submitted to GenBank under accession number OR414381. A phylogenetic tree was generated from the alignments using the neighbor-joining method, and the reliability of the inferred tree was checked with a bootstrap test using the MEGA11 program (Fig. S1).

2.4. Immobilizing strain F4 on biochar J400

Strain F4 was inoculated into 100 mL of Luria-Bertani culture (LB) for 8 h to reach the logarithmic phase and then centrifuged (5000 rpm) for 15 min. The centrifuged deposit was washed with 100 mL sterile 0.9% NaCl three times to remove the carbon source. After that, strain F4

was resuspended in 20 mL 0.9% NaCl and adjusted to OD_{600nm} = 0.40. Biochar (0.5 g) was added to the bacterial suspension and placed in an oscillating incubator (180 rpm) for 5 h for immobilization (Shen et al., 2022). After air drying, the immobilized strain was transferred into a sterile sample bottle labeled as IM and stored at 4 °C.

The number of F4 strains in the suspension (OD_{600nm} = 0.40) was determined using flow cytometry (as detailed in Section 2.6.3) and labeled as *Tt*. Subsequently, free bacteria (*Tu*) were isolated via filtration, and the bacteria immobilized on the biochar were recorded as *Ti*. (*Ti* was calculated as *Ti* = *Tt* - *Tu*), and the bacterial immobilization rate on the biochar (*Tr*) was calculated as *Tr* = (*Ti* / *Tt*) * 100%.

2.5. Bioremediation of petroleum-contaminated soil by immobilized strain F4 on the biochar J400

Three treatments were conducted, and each microcosm was prepared in triplicate with 0.5 kg of soil. (1) CK: 0.22 g KH_2PO_4 and 0.71 g NH_4NO_3 were added to 0.5 kg of petroleum-contaminated soil (2) M: the free strain F4 was inoculated to 0.5 kg of petroleum-contaminated soil and to obtain a density of $4E+7$ cells/g soil, and 0.22 g KH_2PO_4 and 0.71 g NH_4NO_3 were added. (3) IMs: the biochar J400 immobilized strain F4 was mixed with the petroleum-contaminated soil sample at a 5:100 (mass ratio), and 0.22 g KH_2PO_4 and 0.71 g NH_4NO_3 were added. All microcosms were incubated at 24 °C for 90 days. Distilled water was added to the soil to maintain 20% soil moisture. The soil was stirred every 3 days for sufficient aeration.

2.6. Determination of key remediation parameters

2.6.1. TPH and hydrocarbon fractions removal

The extraction of TPH according to the EPA 3550 C (EPA, 2007) method and determined using the gravimetric method for quantification [11,29,30,54]. Specifically, 5 g of dry soil was dispersed in 25 mL of

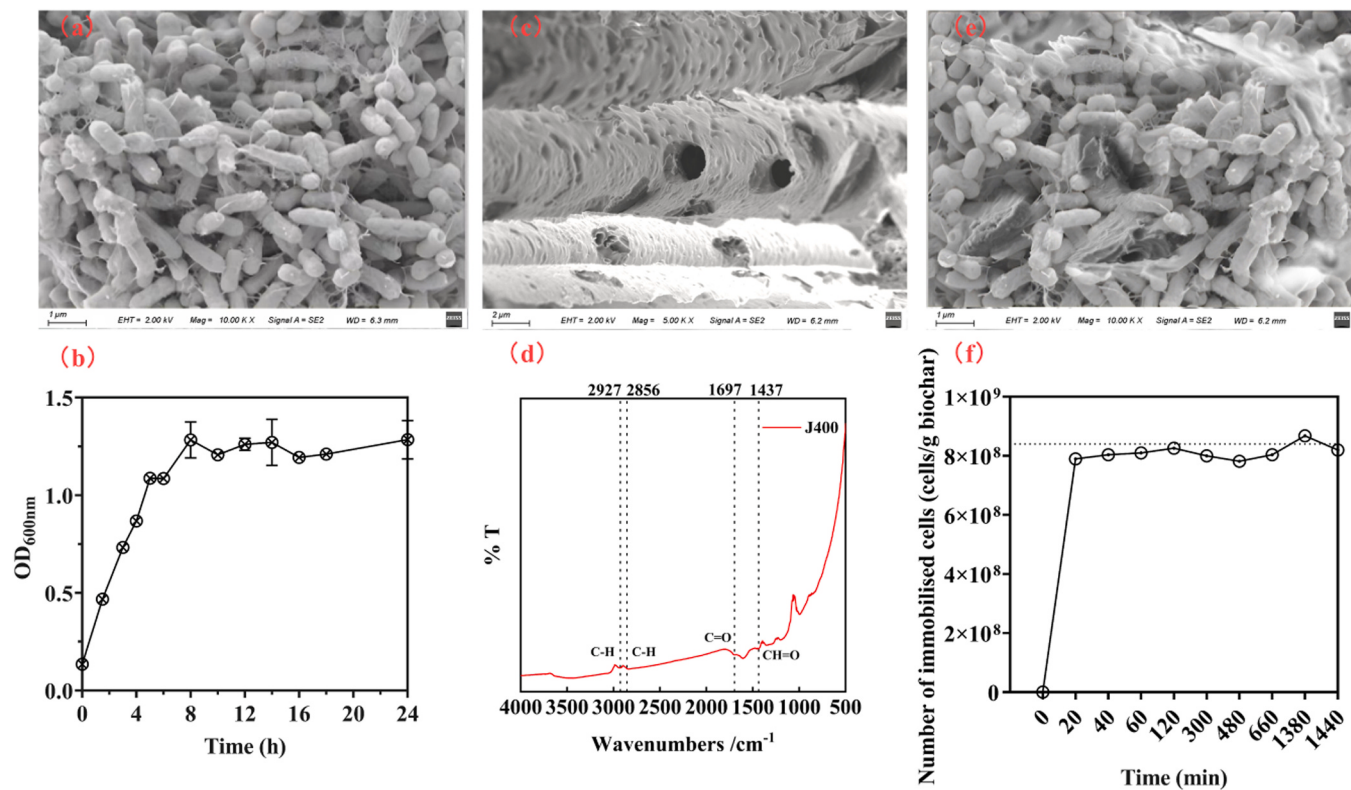


Fig. 1. Scanning electron microscopy (SEM) image of the *Serratia* sp. F4 at the 10,000 × magnification (a), the growth curves of the *Serratia* sp. F4 (b). Surface morphology (c) and FTIR spectroscopy (d) of the biochar J400. SEM magnifications of biochar-immobilized *Serratia* sp. F4 at a 10,000 × magnification (e), and the quantification of strain F4 immobilized on J400 (f).

organic solvent ($V_{(n\text{-hexane})} : V_{(\text{methylene chloride})} = 1:1$). Then, TPH was extracted using an ultrasonic ice bath (JY96-IIN, Ningbo Science Biotechnology Co. LTD, China) and centrifuged at 8000 rpm for 15 min. After filtration, the extracts were dried over Na_2SO_4 , collected in the 30×60 pre-weighed weighing bottle (with a weight of m_1), and dried in a fume hood to evaporate the solvent. The extraction steps were repeated four times to obtain a complete TPH extraction. Finally, after all solvent had evaporated, the mass of the weighing bottle including the extract, was measured and denoted as m_2 . The mass of extractable TPH was determined using the following equation: $m_{\text{TPH}} = m_2 - m_1$ [23]. The biodegradation of TPH in the soil was fitted using a first-order kinetics model ($C_t = C_0 e^{-kt}$), and the half-life ($T_{1/2}$) value of TPH was calculated as $T_{1/2} = \ln 2 / |k|$. C_0 and C_t are the initial amount of TPH and the amount of TPH at time t (mg/kg), respectively. The slope value (k) represents the degradation rate constant (d^{-1}), and t represents the time (days) [32,33].

The saturated hydrocarbons (SHC) and aromatic hydrocarbons (AH) were separated from the TPH by column chromatography using the following procedure: the TPH was dissolved in 5 mL n-hexane, and the saturated and aromatic fractions were then separated using Super Flash Alumina Neutral columns (SF 15–24 g, 20.8 × 112 mm, Agilent Technologies) by employing 5 mL n-hexane and 5 mL benzene as elution solutions, respectively. This procedure was repeated five times. The combined extracts were subsequently dried in a chemical fume hood to evaporate the solvent, and the saturated and aromatic components were measured gravimetrically (Aleksic et al., 2007; [13]).

2.6.2. Soil physicochemical parameters

Soil pH, moisture content, available phosphorus (AP), ammonium nitrogen ($\text{NH}_4^+ \text{-N}$), nitrate nitrogen ($\text{NO}_3^- \text{-N}$), and oxidation-reduction potential (ORP) were measured according to Soil Analysis Technical Specifications (2014).

2.6.3. Total and highly active soil microorganisms

The total numbers of soil microorganisms and highly active cells during bioremediation were determined using the flow cytometer (Accuri C6, BD, USA). The method for extracting total soil microorganisms was modified from a previous study by Lindahl et al. (1996). First, 1 g of soil was added to 9 mL of sterile PBS, and then the culture was shaken at 180 rpm for 30 min in a shaking incubator with gentle agitation every 10 min. Subsequently, the solution was allowed to settle for 10 min. Finally, 2 mL of the supernatant bacterial suspension was collected and filtered through a 5-micron filter. Microbial activity was detected by measuring the membrane integrity using SYBR Green I (SG) and PI staining solutions [51]. Then, 1 mL of bacterial suspension, 445 μL of ultrapure water, and 5 μL of SG/PI staining solution were placed in a 2 mL centrifuge tube. The mixture was agitated for 15 s and incubated in a thermostatic metal bath at 35 °C for 15 min in the dark before performing the fluorescence detection. The FSC and FL1 fluorescence channels were utilized in flow cytometry to assess membrane permeability and obtain total cell counts (TC) and the number of highly active cells (AC) [26].

2.6.4. Soil enzyme activities analysis

Soil dehydrogenase (SDHA) and catalase (CAT) levels were determined using reagent kits with catalog numbers YX-C-B937 and YX-C-B906, respectively, from Shanghai Yuanxin Biotechnology Co., Ltd.

2.6.5. Soil functional gene abundances analysis

Three alkane degradation genes (*alkM*, *Am*, and *CYP*), two polycyclic aromatic hydrocarbon (PAH) degradation genes (*AJ025* and *xylX*), and six nitrogen cycle functional genes (*AOA*, *AOB*, *nrf*, *norB*, *nirK*, and *nosZ*) were detected in the soil samples using quantitative polymerase chain reaction (qPCR). Initially, total DNA was extracted from 0.25 g of soil using the TIANamp Soil DNA Kit (DP336, TIANGEN Biotech Co., Ltd, China). The 20 μL reaction mixture contained 5 μL of soil DNA template,

10 μL of 2 × SYBR green mix II from Sangon Biotech Co., Ltd, China, 4 μL ddH₂O, and 0.5 μL of 10 mM forward and reverse primers (shown at Table S2 and 3). The thermocycling conditions were as follows: initial denaturation at 95 °C for 10 min, 40 cycles at 95 °C for 10 s, with primer annealing at the temperature indicated in Table S2 and 3 for 15 s, and extension at 72 °C for 10 s qPCR assays were performed using a real-time quantitative PCR detection system iQ5 (Bio-Rad, USA) per Wu et al. [55].

2.6.6. Microbial community composition

The initial petroleum-contaminated soil (IS) and soil samples from the CK, M, and IMs microcosms were collected on days 30 and 90 for MiSeq sequencing. DNA was extracted using a Power Soil DNA Extraction Kit (Mo Bio Laboratories, USA). The DNA quality was determined using a 0.5% agarose gel. Bacterial community structure analysis was conducted by amplifying the universal V3-V4 region. Subsequently, the PCR products were loaded onto the Illumina MiSeq platform, following the manufacturer's protocol. After sequencing, data was collected and processed by Sangon Biotech Co., Ltd ([ftp://ftp.sangon.com:21148](http://ftp.sangon.com:21148)). The UPARSE program was used to further analyze the operational taxonomic units (OTUs) and determine the soil microbial community richness and diversity (ACE, Chao1, Shannon, and Simpson indices). Through comparisons with the Greengenes database (<http://greengenes.secondgenome.com>), OTUs were categorized into several bacterial taxa, and the predominant phyla and genera were chosen to illustrate the soil bacterial community profiles.

2.7. Data analysis

All experiments were conducted in triplicate. The experimental results of the TPH content, soil pH, AP, $\text{NH}_4^+ \text{-N}$, $\text{NO}_3^- \text{-N}$, ORP, AC, TC, and enzyme activities were presented as the mean ± standard deviation (SD). Pearson's correlation coefficient using SPSS 25 (Statistical Package for the Social Sciences, China) was calculated to investigate the relationship between petroleum hydrocarbon degradation and soil physicochemical characteristics. A *p*-value < 0.05 was considered statistically significant. A network analysis was performed to examine the connections among microbial species (relative abundance > 0.1%). Spearman's correlation coefficients for pairwise soil microbial taxa were calculated using the Hmisc package (*p* < 0.05), and the networks were visualized using R software v.3.3.1. The robustness of the microbial network was determined by calculating the natural connectivity of the network by removing the nodes in R v.3.3.1.

3. Results and discussion

3.1. Characteristics and morphology of the *Serratia* sp. F4 OR414381, biochar J400, and the biochar J400 immobilized bacteria strain F4

The SEM images revealed that the diameter of the *Serratia* sp. F4 OR414381 ranged from 0.8–1.2 μm (Fig. 1a). The growth curve (Fig. 1b) implied that F4 grew rapidly and reached the logarithmic phase after 8 h of incubation in LB medium. In the liquid-phase system, the degradation efficiency of TPH by strain F4 was 45.5% which indicated the degrader has potential for oil degradation (Fig. S2).

The morphology of the biochar J400 was measured using SEM (Fig. 1c). The surface of biochar J400 was rough and exhibited numerous small spherical structures. FTIR analysis revealed that J400 contains basic functional groups. The absorption peaks at 2927 and 2856 cm^{-1} indicate the presence of aliphatic C-H stretching vibrations in biomacromolecules such as cellulose. Vibrational absorption peaks were observed at 1697 and 1437 cm^{-1} corresponding to the stretching vibrations associated with the aromatic C=O and CH=O bonds (Fig. 1d).

The immobilization rate of strain F4 by biochar J400 reached 89.9% within 20 min in this study (Fig. 1f). After 2 h, the immobilization

efficiency reached a stable level, with biochar J400 achieving high rates (90.18%–96.22%) after 6 h. This indicated that biochar J400 served as an effective immobilization carrier.

3.2. TPH degradation by biochar J400 immobilized *Serratia sp. F4 OR414381* in oil-polluted soil

The initial TPH content of the contaminated soil was 10,133 mg/kg. After 90 days of remediation, TPH content decreased to 3913, 3667, and 1773 mg/kg in the CK, M, and IMs treatments (Fig. 2a), which corresponded to TPH removal efficiencies of 61.38%, 63.81%, and 81.94%, respectively. The IMs treatment was more effective for petroleum degradation than the CK and M treatments.

The TPH removal rate conformed to pseudo-first-order kinetic characteristics (Fig. 2b). The degradation kinetic rate constants (k_{obs}) were 0.0105, 0.0106, and 0.0186 d⁻¹ for the CK, M, and IMs treatments, respectively. The TPH removal rate decreased from 0.011 d⁻¹ at 0–30 days to 0.007 d⁻¹ at 30–90 days in the CK treatment, 0.015 d⁻¹ (0–30 days) to 0.006 d⁻¹ (30–90 days) for the M, and 0.017 d⁻¹ (0–30 days) to 0.010 d⁻¹ (30–90 days) for the IMs treatments (Fig. 2c).

The SHC and AH contents of the soil samples are shown in Fig. 2d. The IMs treatment exhibited a 90.1% SHC reduction (from 7480 to 740 mg/kg) and a 59.23% AH reduction (from 1840 to 740 mg/kg). The removal of AH during IMs treatment (59.2%) was significantly higher compared to the M (24.5%) and CK (22.3%) treatments (Fig. 2f). The IMs treatment also resulted in a greater removal of SHC (Fig. 2e).

Ren et al. [38] employed straw biochar to immobilize bacteria for

remediation of petroleum-contaminated soil, achieving a 48% of TPH remediation efficiency, which was 6% higher than that of free bacteria inoculation. Guo et al. [16] utilized wheat bran biochar to immobilize microbial communities, resulting in a 58% petroleum removal efficiency, surpassing free bacteria inoculation by 14%. Ali et al. (2021) applied sugarcane bagasse biochar with *Enterobacter sp.* MN17 for the remediation of diesel-contaminated soil. The combined TPH removal efficiency was 69%, which was 10% higher than that of free bacteria inoculation. In our study, the IMs treatment exhibited an 18.13% higher petroleum removal efficiency compared to the M treatment ($p = 0.03$). The highest TPH degradation efficiency by the IMs treatment may be attributed to the adaptation of microbes due to the immobilization on the biochar, resulting in increased microbial activity within a short timeframe [39,60,65]. In contrast, direct inoculation with strain F4 may lead to antagonistic effects on indigenous microorganisms, resulting in degradation rates that are not significantly different from those of the control (Curiel et al., 2022).

3.3. Soil NH₄⁺-N, NO₃-N and AP content

The NH₄⁺-N content in treatment M decreased rapidly from 391.4 to 100.3 mg/kg after 10 days of incubation (Fig. 3a). In the IMs-treated soil, the NH₄⁺-N content was consistently higher than in the M treatment. After 90 days of remediation, the NH₄⁺-N contents in the CK, M, and IMs treatments were 3.15, 1.32, and 8.12 mg/kg, respectively. After 90 days of remediation, the NO₃-N content decreased from 462 mg/kg to 81.41, 78.94, and 138.94 mg/kg in the CK, M, and IMs treatments,

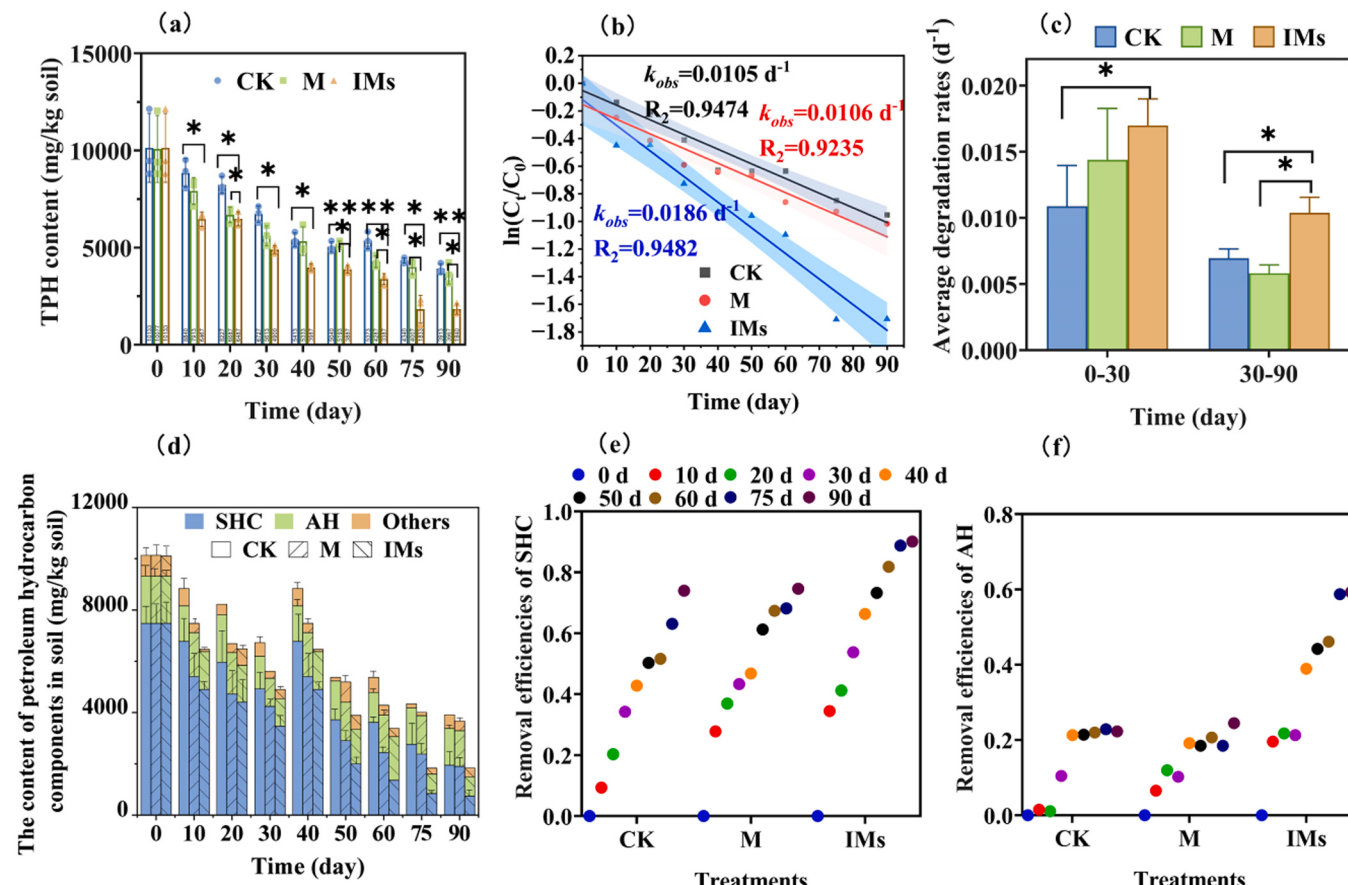


Fig. 2. The TPH content (a), TPH degradation kinetics equation (b), degradation rate for the first thirty days and the subsequent sixty days (c) in the petroleum-contaminated soil. The contents of the hydrocarbon composition including the saturated hydrocarbons (SHC) and others, the aromatic hydrocarbons (AH) (d), the removal efficiencies of SHC (e) and AH (f) in the petroleum-contaminated soil. Errors bars indicate \pm SD of triplicate samples. Different letters in the same time represent a significant difference at $p < 0.05$. The mark "*" and "**" over the determined time respectively indicates the significant difference among different treatments at $p \leq 0.05$ and $p \leq 0.01$ calculated by one-way analysis of variance (ANOVA).

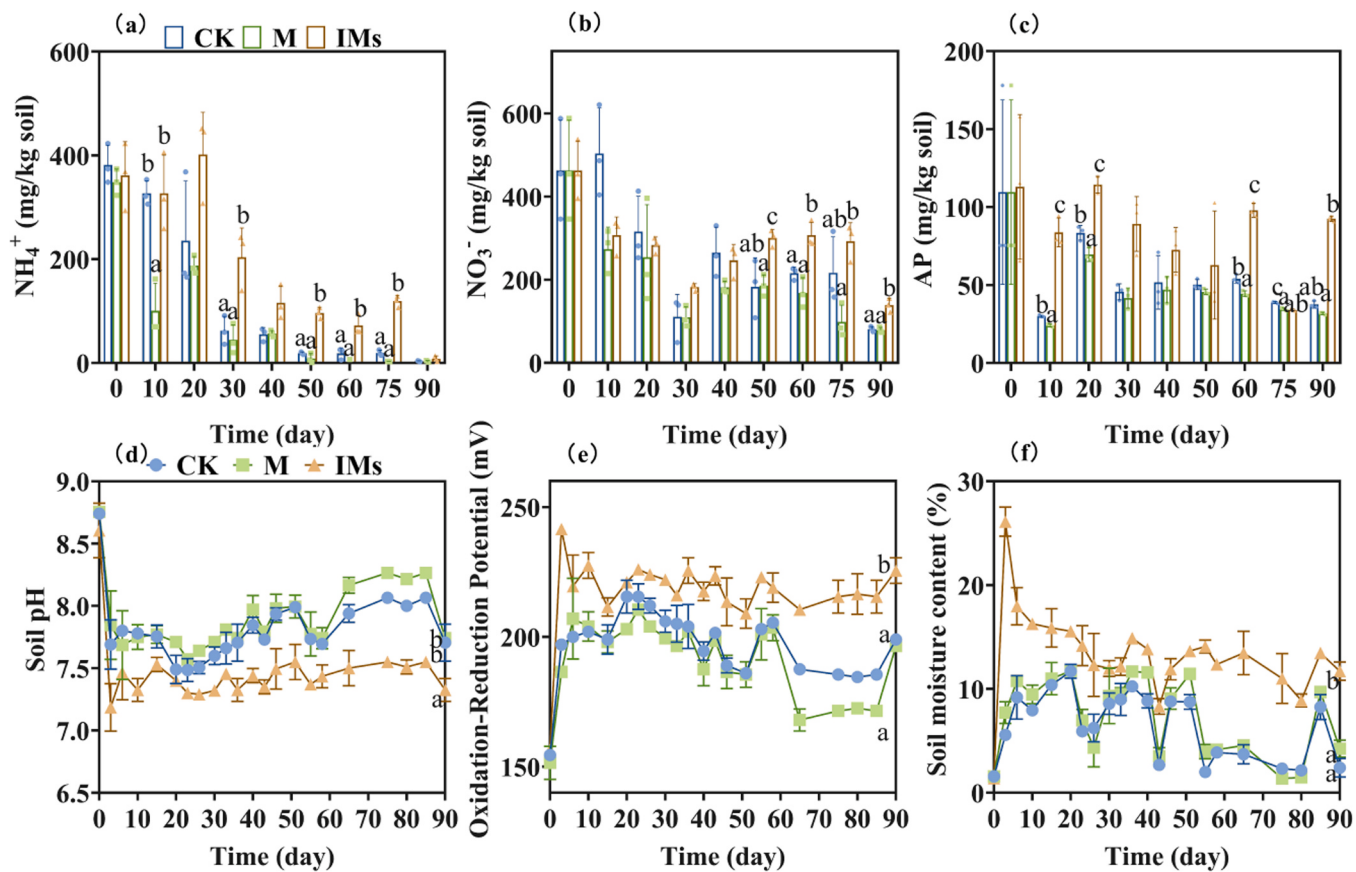


Fig. 3. The changes of NH_4^+ -N (a), NO_3^- -N (b), available phosphorus (c) content, soil pH value (d), ORP (e), and soil moisture content (f) in different treated oil-petroleum soils.

respectively. The NO_3^- -N content in the IMs-treated soil was higher than in the other treatments. The initial AP content of the oil-contaminated soil was 109.6 mg/kg. After 10 days of incubation, the AP content rapidly decreased to 30.05, 24.12, and 83.77 mg/kg in the CK, M, and IMs, respectively. The AP contents were 37.53, 31.77, and 92.47 mg/kg in the CK, M, and IMs treatments, respectively.

This may involve the microbial utilization of inorganic nutrients for substantial growth and the removal of petroleum hydrocarbons from the soil [7,62]. In agriculture, the application of biochar can reduce nitrogen and phosphorus loss in field drainage through a series of effects [45,63] which corresponded to our findings.

3.4. Soil pH, ORP, and moisture content

The initial pH of the oil-contaminated soil was 8.76, indicating alkaline conditions. After 90 days of incubation, the pH values in the CK, M, and IMs treatments were 8.07, 8.27, and 7.55, respectively (Fig. 3d). Soil ORP values for the CK, M, and IMs treatments were 204, 193, and 226 mV (Fig. 3e). This indicates that the biochar-immobilized microorganisms modified the oxidizability of the soil and improved the soil pH to neutral. IMs treatment maintained 11.29% moisture content, demonstrating a commendable ability to regulate soil moisture. It exhibited a remarkable 5.95-fold and 2.7-fold increase compared with the CK and M treatments, respectively. Soil moisture content ($r = 0.88$ and 0.98) emerged as the most significant factor, displaying positive correlations with the axis during the initial 30 days, and 30–90 days of incubation (Fig. 5e and f).

Li et al. [24] reported that the biodegradation of petroleum hydrocarbons produces acidic metabolites that decreases soil pH toward neutrality. The increase in ORP can be attributed to the enhanced soil aeration facilitated by biochar (Song et al., 2015). The porous structure

of biochar contributes to the retention of nutrients and water in soil. Enhanced moisture retention promotes the growth and activity of soil microbes, which play a significant role in soil health and remediation [47].

3.5. Soil microbial quantity and enzyme activity

The number of soil microorganisms was determined using flow cytometry, and scatter plots are shown in Fig. S3. The number of microorganisms in all treatments initially increased, followed by a decrease over the 90-day remediation period. The CK treatment had a maximum total cell counts (TC) of 3.29×10^8 cells/g soil at 20 days, 14.3 times that in the initial soil (Fig. 4a). In treatment M, the maximum TC was 3.54×10^8 cells/g soil. After 30 days of remediation, the TC in the IMs-treated soil reached 1.01×10^9 cells/g soil, exhibiting a 4.65-fold increase compared with the M treatment. The number of highly active cells (AC) reached 7.75×10^8 cells/g soil, representing a 4.84-fold increase compared with that in the M treatment (Fig. 4d and e). This implied that the biochar J400 immobilized strain F4 effectively stimulated microorganism proliferation. This may be attributed to the porous structure of biochar, which provides attachment sites and favorable habitats for microorganism survival, facilitating the enrichment of specific functional groups and the augmentation of biological activity [35]. Concurrently, it encapsulates the introduced degrader, which is shielded by biochar and fosters augmented synergistic interactions with native microorganisms [56].

CAT and SDHA in petroleum-contaminated soils were assessed at 0, 30, 60, and 90 days after treatment (Fig. 4c and f). Regarding CAT activity, the IMs treatment exhibited the highest level after 90 days of incubation and reached 64.24 U/g. The CAT activities in the CK and the M treatments were 48.02 and 57.13 U/g, respectively. This indicated

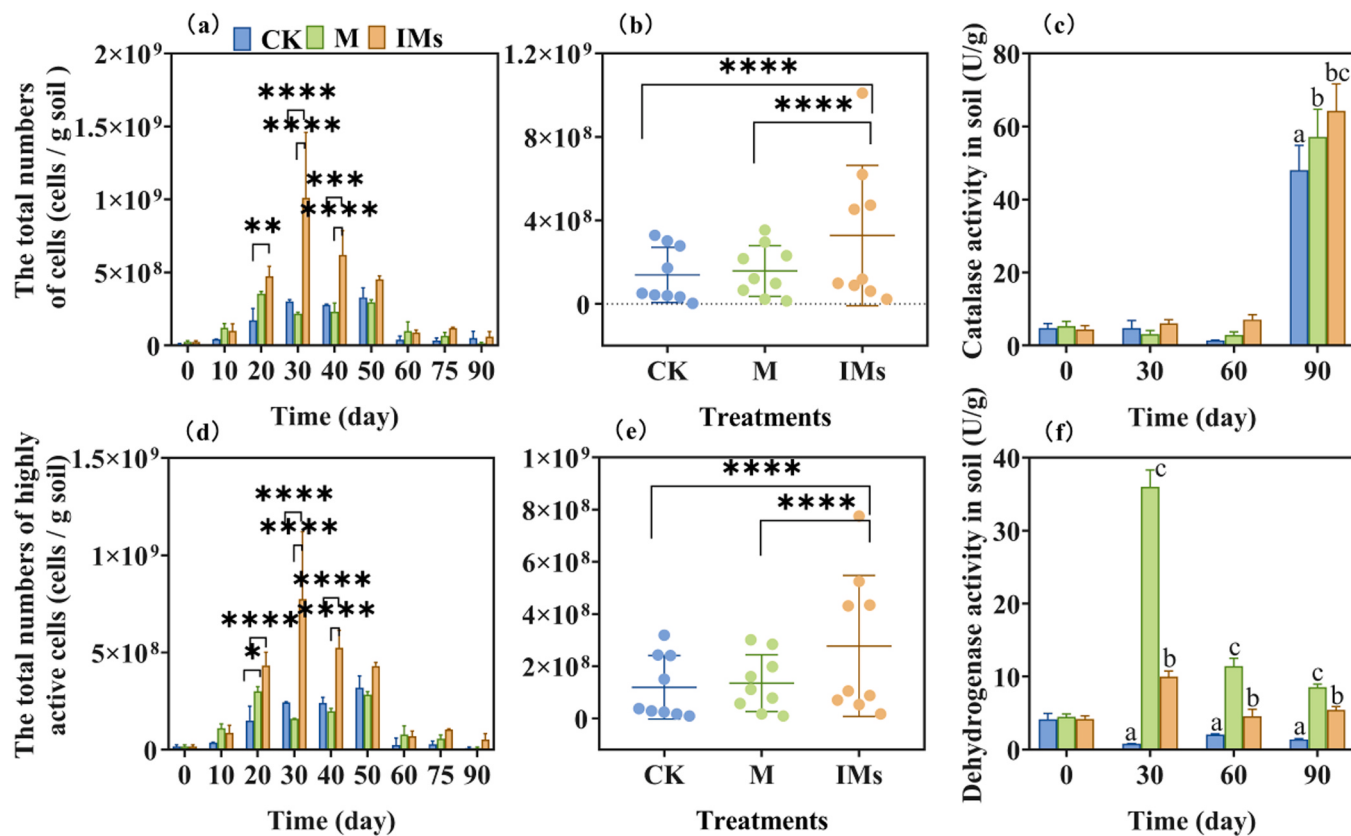


Fig. 4. The numbers of total cells (a, b) and highly active cells (d, e) in the different treated oil-contaminated soils; Soil catalase (c) and dehydrogenase (f) activities of different treatments during remediation time.

that both the IMs and M treatments significantly enhanced CAT levels in petroleum-contaminated soil. CK consistently maintained lower levels of SDHA. However, in the M and IMs treatments, SDHA peaked at 36 and 10 U/g, respectively, after 30 days of remediation. These results indicate that inoculation with J400-immobilized F4 promoted SDHA and CAT in the soils.

3.6. Functional genes of encoding petroleum hydrocarbon degradation and nitrogen-cycling

3.6.1. Functional gene abundances of encoding hydrocarbon degradation

The abundance of petroleum hydrocarbon degradation genes (*Am*, *alkM*, *AJ025*, *xylX*, and *CYP450*) in the CK, M, and IMs treatments are shown in Fig. 5a. In all treatments, the abundance of *CYP450* and *AJ025* was approximately 4–12 orders of magnitude higher than that of *Am*, *alkM*, and *xylX* genes. In the CK treatment, the gene abundances of *CYP450* and *AJ025* were $2.29E+11$ and $4.10E+11$ copies/g soil, respectively (Fig. S4). Compared to the CK treatment, the direct inoculation of degraders (M treatments) resulted in a $7.11E+05$ -fold increase in *CYP450* gene abundance, a $7.06E+05$ -fold increase in *AJ025* gene abundance, and a $2.77E+05$ -fold increase in *xylX* gene abundance, with respective values of $3.09E+16$, $3.17E+17$, and $2.08E+12$ copies/g soil. Compared with the M treatment, the immobilized strain F4 treatment further increased the abundance of *CYP450*, *AJ025*, and *xylX* genes by 1.9, 1.09, and 1.16 times, with values of $3.09E+16$, $3.17E+17$, and $2.08E+12$ copies/g soil, respectively ($p < 0.05$). This indicated a distinct improvement in the *CYP450*, *AJ025*, and *xylX*-harboring communities. Furthermore, the abundance of genes related to alkane degradation exceeded that of genes associated with polycyclic aromatic hydrocarbon degradation. This indicated a greater potential for the degradation of saturated compounds than for aromatic compounds [52].

Redundancy analysis (RDA) of environmental factors and functional

degradation genes revealed an enhanced correlation between AC and TC in soils and displayed a positive correlation with *xylX*, *AJ025*, and *CYP450* ($r > 0.7$), which presented a particularly significant positive correlation observed during the initial 30 days of incubation (Fig. 5e). This may explain why the degradation rate in the first 30 days was higher than that in the subsequent 60 days. However, after 60 days of remediation, TPH showed a strong correlation ($r > 0.7$) with *Am* and *alkM*, whereas the correlation with functional genes explaining other petroleum hydrocarbons decreased.

3.6.2. The abundance of nitrogen-cycling genes

The abundances of nitrogen-cycling genes in the CK treatment varied as *AOA* > *nrf* > *nosZ* > *nirK* > *AOB* > *norB* (Fig. 5a). The abundance of the *nrf* and *AOA* genes significantly increased in the CK treatment compared to the IS, with values of $6.69E+11$ and $1.95E+13$ copies/g soil (Fig. S5). Direct inoculation with strain F4 resulted in a 4.05-fold increase in *AOA* gene abundance, a 2.08-fold increase in *AOB* gene abundance, and a 2.72-fold increase in *nosZ* gene abundance, with values of $7.90E+13$, $7.94E+05$, and $3.23E+11$ copies/g soil, respectively, compared with the CK treatment. The immobilized strain F4 treatment further increased the abundance of *AOB*, *nosZ*, and *norB* genes by 2.61, 2.75, and 1.04 times, with values of $2.08E+06$, $8.28E+11$, and $1.73E+03$ copies/g soil, respectively. However, the IMs treatment resulted in a 56% reduction in *nirK* and an 80% reduction in *AOA* gene abundance compared to the M treatment.

AOA and *AOB* contributed to ammonia oxidation reactions during the first and rate-limiting steps of nitrification in various environmental systems [57]. The highest abundance of *AOA* indicated a favorable environment for nitrification, which could explain the predominance of NO_3^- -N over NH_4^+ -N (Fig. 3). Other investigated nitrogen-cycling genes encode a series of reductases that catalyze denitrification. For instance, *nrf*, *norB/nirK*, and *nosZ* contribute to reducing NO_2^- -N to NH_4^+ -N, NO_2^- -N

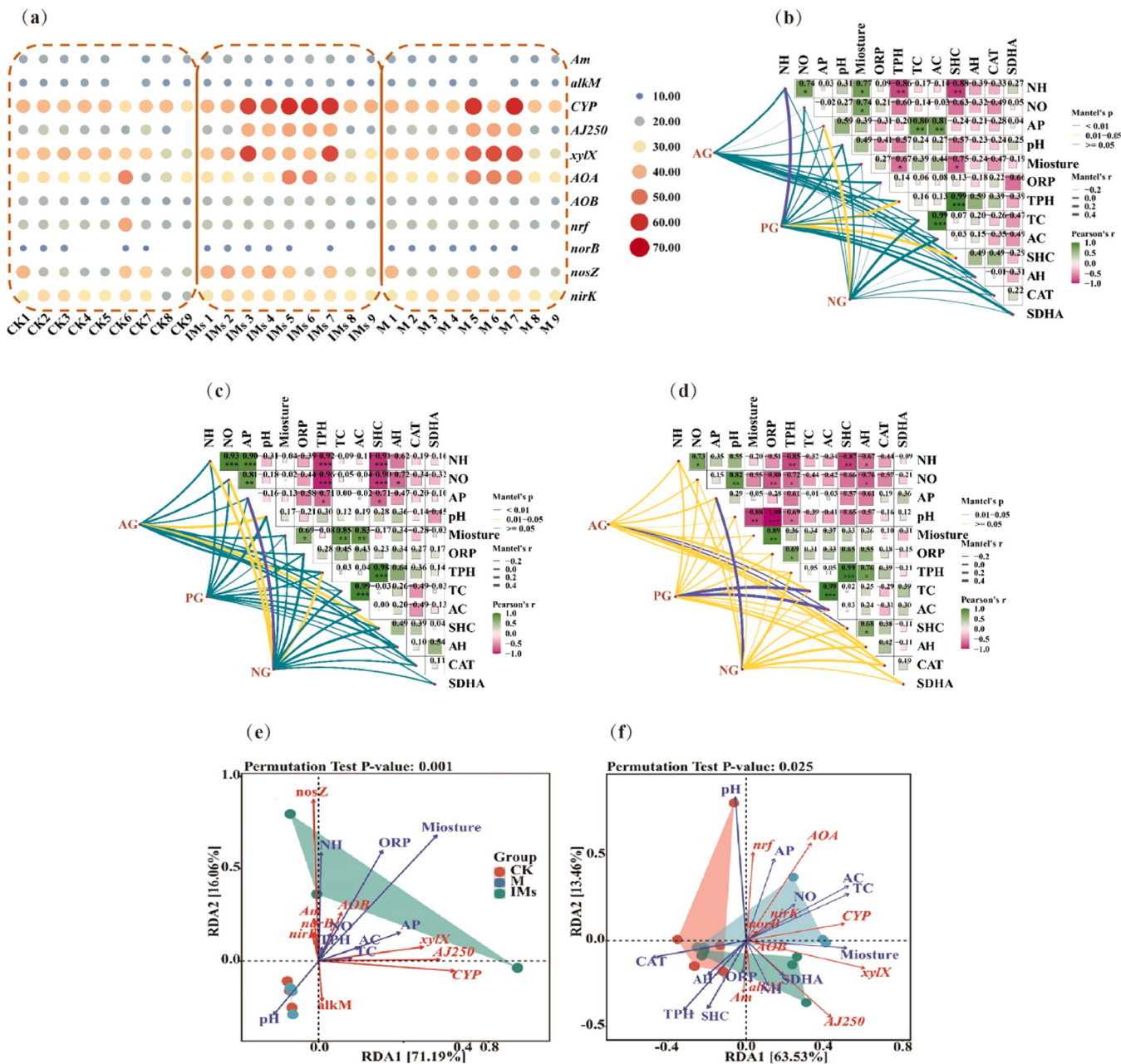


Fig. 5. Heat map illustrating the abundance of soil functional gene copies (a); Functional genes and environmental factors in CK (b), M (c), and IMs (d) treatments. Redundancy analyses depict the relationship between soil physicochemical properties and functional genes during two incubation periods: the initial 30 days (e) and days 30 to 90 (f). The asterisk represents the significant difference ($p < 0.05$). (Abbreviations: NH: NH_4^+ -N; NO: NO_3^- -N; AP: Available phosphorus; TC: total number of cells in soil; AC: highly active cells in soil; AG: Alkane degradation functional genes; PG: Polycyclic aromatic hydrocarbon degradation functional genes; NG: Nitrogen cycle functional genes.).

to NO, and N_2O to N_2 , respectively (Li et al., 2023). The response of denitrification genes (except *nrf*) to the addition of strain F4 showed an increasing trend, and the IMs treatment also exhibited a similar change.

Heat maps displaying the correlations between the soil functional genes and environmental factors are shown in Fig. 5b, c, and d. When comparing the CK and M treatments, the positive correlations of soil AC and AH and the positive correlations of soil moisture and the removal of SHC and AH were strengthened in the IMs treatment. According to the Mantel analysis, the abundance of alkane monooxygenase functional genes (AG) significantly affected AC ($r = 0.23$, $p < 0.01$) and SHC degradation, and the dioxygenase functional genes (PG) influenced AC and TC ($r > 0.35$, $p < 0.01$). This indicated that the effective promotion of petroleum hydrocarbon degradation primarily resulted from

maintaining soil moisture, facilitating the growth of petroleum hydrocarbon-degrading bacteria, and ultimately leading to higher degradation rates in the IMs treatment than in the others.

Concurrently, our findings revealed that during the initial 30 days, *nirk*, *norB*, *AOB*, and *nosZ* were correlated with TPH degradation (Fig. 5e). Conversely, after subsequent 60 days of remediation, a negative correlation ($-0.3 < r < -0.9$) was evident between soil nitrogen-cycling and petroleum degradation (Fig. 5f). Moreover, the positive correlation between AC, TC, and nitrogen-cycling functional genes increased. This suggested that nitrogen-cycling within the first 30 days positively influenced petroleum degradation. However, in the subsequent 60 days, the declining microbial population and a shift toward nitrogen-cycling contributed to the diminished degradation efficiency.

3.7. Changes in soil microbial community structures

Alpha diversity was used to assess the richness and diversity of the microbial communities, and the results are presented in Table 2. The maximum number of OTUs was 1772 on day 0 and gradually decreased on days 30 and 90 across the various treatments. Specifically, the M treatment exhibited higher OTUs of 1445 and 1249 on days 30 and 90, respectively, whereas CK had the lowest OTUs values at 1445 and 1249 on days 30 and 90, respectively.

Analysis of the Chao 1 and Ace indices revealed that their peak values on day 0 were 1858.2 and 1911.0, respectively. Notably, both the M and IMs treatments exhibited higher Chao 1 and Ace indices than the CK treatment. These findings suggest that the introduction of free strain F4 and biochar-immobilized strain F4 increased the abundance of microbial communities.

In the contaminated initial soil (IS), *Actinobacteria* and *Proteobacteria* were the dominant phyla, with relative abundances of 43.96% and 37.51%, respectively. The *Acidobacteria* phylum was the subdominant accounting for 8.22% (Fig. 6a). At the class level, the dominant classes were *Actinobacteria* (40.64%) and *Alphaproteobacteria* (22.20%) (Fig. 6b). The dominant genera were *Nocardia* (28.52%) and *Sphingomonas* (4.07%) (Fig. 6c).

After 90 days of incubation, the microbial community composition changed in the CK treatment. The relative abundance of the *Actinobacteria* phylum increased to 44.63%, whereas the abundances of *Proteobacteria* and *Acidobacteria* phyla decreased to 26.50% and 1.03%, respectively. At the genus level, *Nocardia* and *Sphingomonas* reduced during remediation with 0.31% and 0.03%, whereas *Rhodococcus* and *Dietzia* exhibited substantial increases of 15.03% and 9.65%, respectively.

The dominant phyla in treatment M were consistent with those in treatment CK. At the genus level, *Nocardia* (0.90%) and *Sphingomonas* (0.03%) decreased during remediation. The microbial community composition changed significantly in the IMs treatment compared to the M treatment. *Proteobacteria* became the dominant phylum, with a relative abundance increased to 40.96% after 90 days of incubation in the IMs treatment. At the genus level, *Salinimicrobium* genus became predominant, accounting for 10.26%, while *Brevundimonas* (1.28%) genus increased and became the dominant genus (Fig. 6c). Reportedly, *Salinimicrobium* synthesize catalase and cytochrome oxidase for hydrocarbon degradation in soil [19,46,6]. *Brevundimonas* has a high tolerance to seawater salinity and can be used in the bioremediation of contaminated soils and water from oil transportation spills [32].

Network co-occurrence analyses of the core genera between the CK, M, and IMs treatments are shown in Fig. 6d, e, and f, respectively. The CK treatment network model consisted of 40 nodes connected by 460 lines, the M treatment network model comprised 40 nodes connected by 558 lines, and the IMs treatment network model consisted of 40 nodes connected by 574 lines. The core species of the three treatment groups were divided into three modules. The positive correlations within bacterial communities were notably observed as 66.5%, 54.6%, and 89.7% in the CK, M, and IMs treatments, respectively, indicating biochar-immobilized strain F4 enhanced mutualistic interactions among soil bacterial communities while mitigating the antagonistic effects imposed by the introduction of strain F4 on the indigenous soil microbiota [31],

which also found by Geng et al. [14]. Introducing the biochar-immobilized *Serratia* sp. F4 into the polluted soil was positively correlated with *Salinimicrobium* in Model I of the IMs treatment. Therefore, adding biochar-J400-immobilized strain F4 enriched microorganisms with similar functions, forms a dominant microbiome with petroleum hydrocarbon degradation capability.

An RDA of environmental factors, petroleum hydrocarbon-degrading bacteria (Fig. 7a), and other microbes (Fig. 7b) revealed that the variations in functional petroleum hydrocarbon-degrading bacteria during the 30–90 days of incubation were not significant. In contrast, the abundance of *Devosia*, *Rhizobiales*, *Mesorhizobium*, and *Sphingoaurantiacus* increased on day 90 (Fig. 7b). In investigations of denitrification systems, *Devosia* was found to participate in ammonia oxidation [52]. *Mesorhizobium* and *Rhizobiales* genera are closely associated with soil nitrogen fixation [12,2,25,27,37,41,43,44,49,5,59,61,64,8]. After 90 days of incubation, the IMs treatment exhibited a notably stronger positive correlation ($r > 0.7$) with the five petroleum hydrocarbon-degrading genes, *Saccharibacteria genera incertae sedis*, *Alcanivorax*, *Brevundimonas*, *Lysobacter*, and *Salinimicrobium*. These degrading bacteria established a beneficial interaction with the immobilized strain F4, consequently promoting the degradation of petroleum hydrocarbons during IMs treatment.

4. Conclusions

This study immobilized petroleum hydrocarbon-degrading bacteria on agricultural waste biochar using a simple and efficient adsorption method and then used the product to remediate crude-oil-contaminated soil. This treatment had several notable effects on soil quality and microbial dynamics. Specifically, remediation using biochar immobilization of *Serratia* sp. F4 OR414381 enhanced soil moisture content, stimulated the growth of native soil microorganisms, and improved interactions and stability within the soil bacterial community. These factors enhance soil dehydrogenase activity and upregulate the expression of functional genes involved in petroleum hydrocarbon degradation. Consequently, this treatment achieved the highest petroleum hydrocarbon degradation efficiency and shortest half-life for petroleum hydrocarbon degradation. Moreover, this treatment demonstrated its capability to prevent the loss of nitrogen and phosphorus.

Environmental implication

Oil pollution is a pressing concern because of its significant threat to soil safety. This study investigated the effectiveness of remediation of petroleum-contaminated soil and changes in soil microbial composition using biochar-immobilized *Serratia* sp. F4 methods. After 90 days of remediation, 82.5% of total petroleum hydrocarbons, 59.23% of aromatic hydrocarbons, and 90.1% of saturated hydrocarbons, were successfully removed. Biochar immobilization significantly promoted the growth of *Serratia* sp. F4 and established a beneficial interaction between indigenous microorganisms and strain F4, simultaneously reducing the loss of soil inorganic nutrients. Biochar-immobilized *Serratia* sp. F4 is an important strategy for reducing petroleum contamination and improving the ecological environment in loess soil.

Table 2

The alpha diversity of microbial communities in contaminated soils at different stages of remediation treatments.

| Soil | IS | 30 d CK | 30d M | 30 d IMs | 90 d CK | 90 d M | 90 d IMs |
|----------|----------|----------|----------|----------|----------|----------|----------|
| OTUs | 1772 | 1412 | 1445 | 1342 | 808 | 1249 | 1242 |
| Shannon | 4.88 | 3.89 | 4.32 | 4.45 | 3.59 | 4.10 | 4.48 |
| Chao1 | 1858.2 | 1566.6 | 1595.0 | 1510.1 | 1047.0 | 1419.7 | 1378.6 |
| Ace | 1911.0 | 1629.1 | 1640.9 | 1567.5 | 1050.0 | 1461.1 | 1451.2 |
| Simpson | 0.075927 | 0.082077 | 0.046647 | 0.036696 | 0.067293 | 0.044023 | 0.02912 |
| Coverage | 0.994852 | 0.994254 | 0.993877 | 0.993789 | 0.996407 | 0.994194 | 0.994235 |

Note: IS: the initial petroleum-contaminated soil

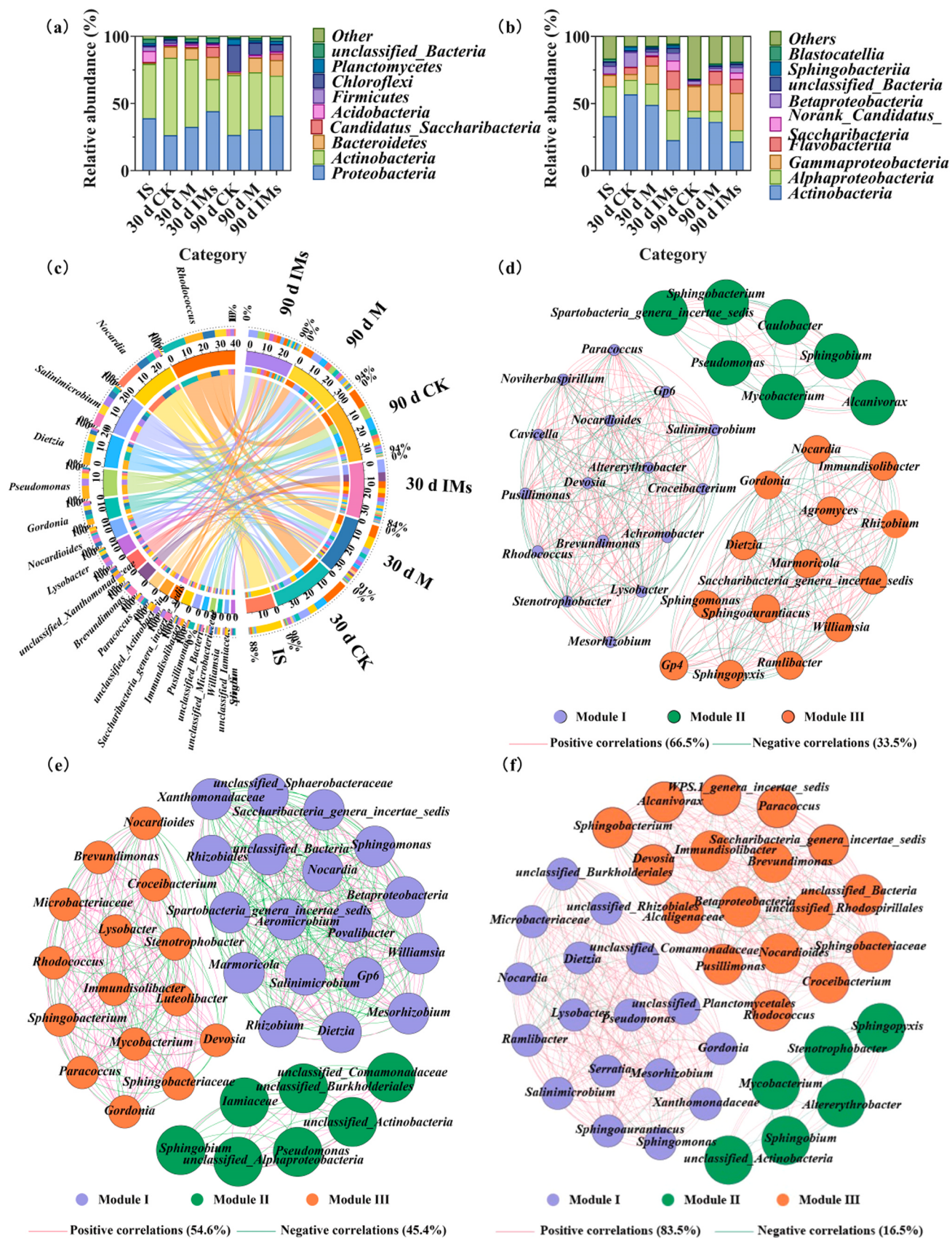


Fig. 6. Microbial community composition at phyla (a), class (b) and genus (c) levels in the different treatments from Illumina sequencing; The network co-occurrence analysis of the core genera among the CK (d), M (e) and IMs (f) treatment.

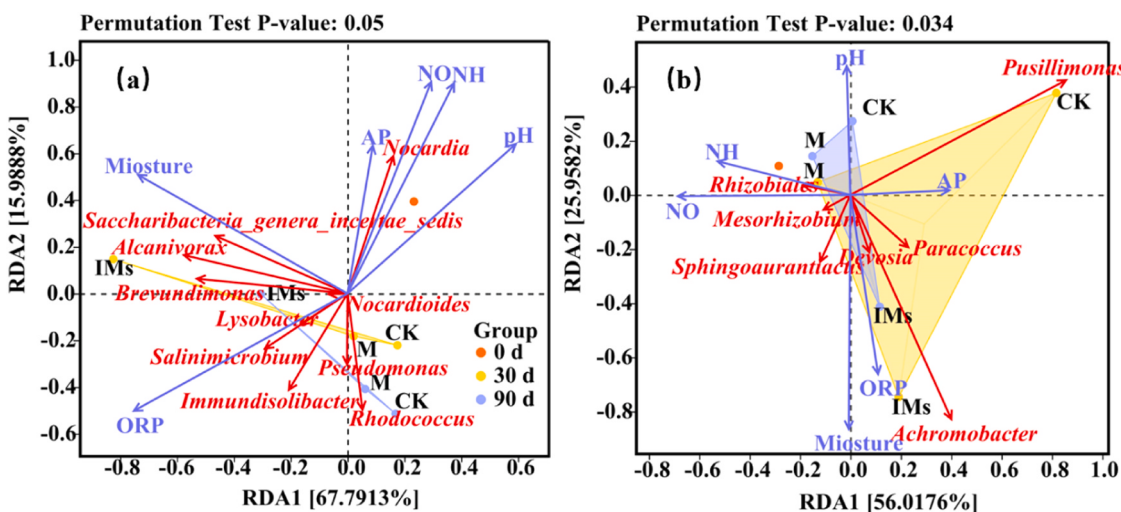


Fig. 7. Major petroleum hydrocarbon-degrading functional genera (a) and other functional genera (b) within the soil 0, 30, and 90 days.

CRediT authorship contribution statement

Huan Gao: Visualization, Methodology. **Yawen Ou:** Validation, Resources. **Mengqi Li:** Methodology. **Xuhong Zhang:** Writing – original draft, Methodology, Formal analysis, Data curation. **Manli Wu:** Writing – review & editing, Validation, Funding acquisition, Conceptualization. **Ting Zhang:** Validation, Resources, Investigation.

Declaration of Competing Interest

The authors declare that they have no known competing financial interests or personal relationships that could have appeared to influence the work reported in this paper.

Data Availability

No data was used for the research described in the article.

Acknowledgments

This work was supported by the National Natural Science Foundation of China (Nos. 52070154) and the Key Research and Development Project of Shaanxi Province, China (2023-YBNY-251).

Appendix A. Supporting information

Supplementary data associated with this article can be found in the online version at [doi:10.1016/j.jhazmat.2024.134137](https://doi.org/10.1016/j.jhazmat.2024.134137).

References

- [1] Ali Khan, A.H., Tanveer, S., Alia, S., Anees, M., Sultan, A., Iqbal, M., Yousaf, S., 2017. Role of nutrients in bacterial biosurfactant production and effect of biosurfactant production on petroleum hydrocarbon biodegradation. *Ecol Eng* 104, 158–164.
- [2] Ali, M., Sattar, M., Khan, M., Naveed, M., Rafique, M., Alamri, S., Siddiqui, M.H., 2020. Enhanced growth of mungbean and remediation of petroleum hydrocarbons by *Enterobacter* sp. MN17 and biochar addition in diesel contaminated soil. *Appl Sci* 10 (23), 8548.
- [3] Ali, S., Rizwan, M., Noureen, S., Anwar, S., Ali, B., Naveed, M., Ahmad, P., 2019. Combined use of biochar and zinc oxide nanoparticle foliar spray improved the plant growth and decreased the cadmium accumulation in rice (*Oryza sativa L.*) plant. *Environ Sci Pollut Res Int* 26 (11), 11288–11299.
- [4] AlKaabi, N., Al-Ghouti, M.A., Jaoua, S., Zouari, N., 2020. Potential for native hydrocarbon-degrading bacteria to remediate highly weathered oil-polluted soils in Qatar through self-purification and bioaugmentation in biofilms. *Biotechnol Rep (Amst, Neth)* 28, 543.
- [5] Apul, O.G., Arrowsmith, S., Hall, C.A., Miranda, E.M., Alam, F., Dahlen, P., Delgado, A.G., 2022. Biodegradation of petroleum hydrocarbons in a weathered, unsaturated soil is inhibited by peroxide oxidants. *J Hazard Mater* 433, 128770.
- [6] Barberán, A., Cáceres Velázquez, H., Jones, S., Fierer, N., Hallam, S.J., 2017. Hiding in plain sight: mining bacterial species records for phenotypic trait information. *Chemosphere* 2 (4).
- [7] Bodor, A., Boudjoum, N., Feigl, G., Duzs, Á., Laczi, K., Szilágyi, Á., Rákely, G., Perei, K., 2021. Exploitation of extracellular organic matter from *Micrococcus luteus* to enhance *ex situ* bioremediation of soils polluted with used lubricants. *J Hazard Mater* 417, 125996.
- [8] Campos, J.A., Peco, J.D., García-Noguero, E., 2019. Antigerminative comparison between naturally occurring naphthoquinones and commercial pesticides. *Soil dehydrogenase activity used as bioindicator to test soil toxicity*. *Sci Total Environ* 694, 133672.
- [9] Chen, B., Yuan, M., Qian, L., 2012. Enhanced bioremediation of PAH-contaminated soil by immobilized bacteria with plant residue and biochar as carriers. *J Soils Sediment* 12 (9), 1350–1359.
- [10] Cocărtă, D., Stoian, M., Karademir, A., 2017. Crude oil contaminated sites: evaluation by using risk assessment approach. *Sustain (Basel, Switz)* 9 (8), 1365.
- [11] Chen, T., Delgado, A., Yavuz, B., Maldonado, J., Zuo, Y., Kamath, R., Westerhoff, P., Krajmalnik-Brown, R., Rittmann, B., E., 2017. Interpreting interactions between ozone and residual petroleum hydrocarbons in soil. *Environ Sci Technol* 51 (1), 506–513.
- [12] Curiel-Alegre, S., Velasco-Arroyo, B., Rumbo, C., Khan, A.H.A., Tamayo-Ramos, J. A., Rad, C., Barros, R., 2022. Evaluation of biostimulation, bioaugmentation, and organic amendments application on the bioremediation of recalcitrant hydrocarbons of soil. *Chemosphere (Oxf)* 307, 135638–135638.
- [13] Gao, S., Liang, J., Teng, T., Zhang, M., 2019. Petroleum contamination evaluation and bacterial community distribution in a historic oilfield located in loess plateau in China. *Appl Soil Ecol* 136, 30–42.
- [14] Geng, P., Ma, A., Wei, X., Chen, X., Yin, J., Hu, F., Zhuang, X., Song, M., Zhuang, G., 2022. Interaction and spatio-taxonomic patterns of the soil microbiome around oil production wells impacted by petroleum hydrocarbons. *Environ Pollut* 307, 119531.
- [15] Govarthanan, M., Liang, Y., Kamala-Kannan, S., Kim, W., 2022. Eco-friendly and sustainable green nano-technologies for the mitigation of emerging environmental pollutants. *Chemosphere* 287 (2), 132234.
- [16] Guo, S., Liu, X., Tang, J., 2022. Enhanced degradation of petroleum hydrocarbons by immobilizing multiple bacteria on wheat bran biochar and its effect on greenhouse gas emission in saline-alkali soil. *Chemosphere (Oxf)* 286, 131663–131663.
- [17] Karthick, A., Roy, B., Chattopadhyay, P., 2019. A review on the application of chemical surfactant and surfactant foam for remediation of petroleum oil contaminated soil. *J Environ Manag* 243, 187–205.
- [18] Kiamarsi, Z., Soleimani, M., Nezami, A., Kafi, M., 2019. Biodegradation of n-alkanes and polycyclic aromatic hydrocarbons using novel indigenous bacteria isolated from contaminated soils. *Int J Environ Sci Technol (Tehran)* 16 (11), 6805–6816.
- [19] Kim, J., Yoon, J., Kim, W., 2016. *Salinimicrobium soli* sp. nov., isolated from soil of reclaimed land. *Int J Syst Evolut Microbiol* 66 (1), 462.
- [20] Kong, F., Sun, G., Liu, Z., 2018. Degradation of polycyclic aromatic hydrocarbons in soil mesocosms by microbial/plant bioaugmentation: Performance and mechanism. *Chemosphere (Oxf)* 198, 83–91.
- [21] Kong, L., Gao, Y., Zhou, Q., Zhao, X., Sun, Z., 2018. Biochar accelerates PAHs biodegradation in petroleum-polluted soil by biostimulation strategy. *J Hazard Mater* 343, 276–284.
- [22] Kour, D., Kaur, T., Devi, R., Yadav, A., Singh, M., Joshi, D., Saxena, A.K., 2021. Beneficial microbiomes for bioremediation of diverse contaminated environments

- for environmental sustainability: present status and future challenges. Environ Sci Pollut Res Int 28 (20), 24917–24939.
- [23] Li, D., Xu, W., Mu, Y., Yu, Q., Jiang, H., John, C., 2018. Remediation of petroleum-contaminated soil and simultaneous recovery of oil by fast pyrolysis. Environ Sci Technol 52 (9), 5330–5338.
- [24] Li, X., Song, Y., Bian, Y., Gu, C., Yang, X., Wang, F., Jiang, X., 2020. Insights into the mechanisms underlying efficient Rhizodegradation of PAHs in biochar-amended soil: from microbial communities to soil metabolomics. Environ Int 144, 105995.
- [25] Liang, Z., Li, G., Mai, B., Ma, H., An, T., 2019. Application of a novel gene encoding bromophenol dehalogenase from *Ochrobactrum sp.* T in TBBPA degradation. Chemosphere 217, 507–515.
- [26] Lin, W., Zuo, J., Li, K., Hu, R., Xu, X., Huang, T., Wen, G., Ma, J., 2023. Pre-exposure of peracetic acid enhances its subsequent combination with ultraviolet for the inactivation of fungal spores: Efficiency, mechanisms, and implications. Water Res 229, 119404.
- [27] Lindahl, V., 1996. Improved soil dispersion procedures for total bacterial counts, extraction of indigenous bacteria and cell survival. J Microbiol Methods 25 (3), 279–286.
- [28] Liu, H., Wu, M., Zhang, M., Gao, H., Yan, Z., Yang, Z., 2023. New insight into the effect of nitrogen on hydrocarbon degradation in petroleum-contaminated soil revealed through ^{15}N tracing and flow cytometry. Sci Total Environ 891, 164409.
- [29] Liu, H., Wu, M., Gao, H., Yi, N., Duan, X., 2021. Hydrocarbon transformation pathways and soil organic carbon stability in the biostimulation of oil-contaminated soil: Implications of ^{13}C natural abundance. Sci Total Environ 788, 147580.
- [30] Liu, Z., Li, Z., Chen, S., Zhou, W., 2023. Enhanced phytoremediation of petroleum-contaminated soil by biochar and urea. J Hazard Mater 453, 131404.
- [31] Ma, B., Zhang, H., Huang, T., Chen, S., Sun, W., Yang, W., Niu, L., Liu, X., Liu, H., Pan, S., Liu, H., Zhang, X., 2023. Aerobic denitrification enhanced by immobilized slow-released iron/activated carbon aquagel treatment of low C/N micropolluted water: Denitrification performance, denitrifying bacterial community co-occurrence, and implications. Environ Sci Technol 57 (13), 5252–5263.
- [32] Ma, L., Hu, T., Liu, Y., Liu, J., Wang, Y., Wang, P., Li, L., 2021. Combination of biochar and immobilized bacteria accelerates polyacrylamide biodegradation in soil by both bio-augmentation and bio-stimulation strategies. J Hazard Mater 405, 124086.
- [33] Ma, M., Gao, W., Li, Q., Han, B., Zhu, A., Yang, H., Zheng, L., 2021. Biodiversity and oil degradation capacity of oil-degrading bacteria isolated from deep-sea hydrothermal sediments of the South Mid-Atlantic Ridge. Mar Pollut Bull 171, 112770.
- [34] Marchand, L., Sabaris, C.Q., Desjardins, D., Oustriere, N., Pesme, E., Butin, D., Mench, M., 2016. Plant responses to a phytomanaged urban technosol contaminated by trace elements and polycyclic aromatic hydrocarbons. Environ Sci Pollut Res Int 23 (4), 3120–3135.
- [35] Nath, H., Sarkar, B., Mitra, S., Bhaladhere, S., 2022. Biochar from biomass: a review on biochar preparation its modification and impact on soil including soil microbiology. Geomicrobiol J 39 (3-5), 373–388.
- [36] Ossai, I.C., Ahmed, A., Hassan, A., Hamid, F.S., 2020. Remediation of soil and water contaminated with petroleum hydrocarbon: a review. Environ Technol Innov 17, 100526.
- [37] Rajakovic, V., Aleksic, G., Radetic, M., Rajakovic, L., 2007. Efficiency of oil removal from real wastewater with different sorbent materials. J Hazard Mater 143 (1), 494–499.
- [38] Ren, H., Wei, Z., Wang, Y., 2020. Effects of biochar properties on the bioremediation of the petroleum-contaminated soil from a shale-gas field. Environ Sci Pollut Res 27, 36427–36438.
- [39] Saeed, M., Ilyas, N., Bibi, F., Shabir, S., Jayachandran, K., Sayyed, R.Z., Rizvi, Z.F., 2023. Development of novel kinetic model based on microbiome and biochar for in-situ remediation of total petroleum hydrocarbons (TPHs) contaminated soil. Chemosphere 324, 138311.
- [40] Saeed, M., Ilyas, N., Jayachandran, K., Gaffar, S., Arshad, M., Sheeraz Ahmad, M., Hessini, K., 2021. Biostimulation potential of biochar for remediating the crude oil contaminated soil and plant growth. Saudi J Biol Sci 28 (5), 2667–2676.
- [41] Shen Ruofei, X.X.T.B., 2022. Remediation of petroleum hydrocarbon contaminated groundwater by biochar immobilized bacterial consortia. Environ Chem 2023 (2023), 9–18.
- [42] Silvani, L., Vrchoťová, B., Kastanek, P., Demnerová, K., Pettiti, I., Papini, M.P., 2017. Characterizing biochar as alternative sorbent for oil spill remediation. Sci Rep 7 (1), 43912–43912.
- [43] Song, J., Wang, B., 2015. Using euhalophytes to understand salt tolerance and to develop saline agriculture: *Suaeda salsa* as a promising model. Ann Bot 115 (3), 541–553.
- [44] Sun, M., Ye, M., Liu, K., Schwab, A.P., Liu, M., Jiao, J., Jiang, X., 2017. Dynamic interplay between microbial denitrification and antibiotic resistance under enhanced anoxic denitrification condition in soil. Environ Pollut 222, 583–591.
- [45] Tan, Z., Yuan, S., Hong, M., Zhang, L., Huang, Q., 2020. Mechanism of negative surface charge formation on biochar and its effect on the fixation of soil Cd. J Hazard Mater 384, 121370.
- [46] Third Institute of Oceanography, M.O.N.R. 2008. MCCC 1A04469 Salinimicrobium 2023-9-3, 2023, from (http://www.nimr.org.cn/Column.asp?Column_ID=334997597&model=product_detail&P_ID=1707203).
- [47] Vijay, V., Shreedhar, S., Adlak, K., Payyanad, S., Sreedharan, V., Gopi, G., Aravind, P.V., 2021. Review of large-scale biochar field-trials for soil amendment and the observed influences on crop yield variations. Front Energy Res 9, 710766.
- [48] Wang, Q., Deng, J., Liang, J., Jiang, L., Arslan, M., Gamal El-Din, M., Chen, C., 2022. Biochar immobilized petroleum degrading consortium for enhanced granulation and treatment of synthetic oil refinery wastewater. Bioresour Technol Rep 17, 100909.
- [49] Wang, X., Wang, X., Liu, M., Zhou, L., Gu, Z., Zhao, J., 2016. Bioremediation of marine oil pollution by *Brevundimonas diminuta*: effect of salinity and nutrients. Desalin Water Treat 57 (42), 19768–19775.
- [50] Wei, Z., Wei, Y., Liu, Y., Niu, S., Xu, Y., Park, J., Wang, J.J., 2024. Biochar-based materials as remediation strategy in petroleum hydrocarbon-contaminated soil and water: Performances, mechanisms, and environmental impact. J Environ Sci (China) 138, 350–372.
- [51] Wen, G., Cao, R., Wan, Q., Tan, L., Xu, X., Wang, J., Huang, T., 2020. Development of fungal spore staining methods for flow cytometric quantification and their application in chlorine-based disinfection. Chemosphere 243, 125453.
- [52] Wu, H., Cui, M., Yang, N., Liu, Y., Wang, X., Zhang, L., Zhan, G., 2022. Aerobic biocathodes with potential regulation for ammonia oxidation with concomitant cathodic oxygen reduction and their microbial communities. Bioelectrochemistry 144, 107997.
- [53] Wu, M., Chen, L., Tian, Y., Ding, Y., Dick, W.A., 2013. Degradation of polycyclic aromatic hydrocarbons by microbial consortia enriched from three soils using two different culture media. Environ Pollut 178, 152–158.
- [54] Wu, M., Dick, W.A., Li, W., Wang, X., Yang, Q., Wang, T., Chen, L., 2016. Bioaugmentation and biostimulation of hydrocarbon degradation and the microbial community in a petroleum-contaminated soil. Int Biodeterior Biodegrad 107, 158–164.
- [55] Wu, M., Liu, Z., Gao, H., Gao, J., Xu, Y., Ou, Y., 2022. Assessment of bioremediation potential of petroleum-contaminated soils from the shanbei oilfield of China revealed by qPCR and high throughput sequencing. Chemosphere 308, 136446.
- [56] Xiang, L., Harindintwali, J.D., Wang, F., Redmile-Gordon, M., Chang, S.X., Fu, Y., Xing, B., 2022. Integrating biochar, bacteria, and plants for sustainable remediation of soils contaminated with organic pollutants. Environ Sci Technol 56 (23), 16546–16566.
- [57] Xiao, Z., Rasmann, S., Yue, L., Lian, F., Zou, H., Wang, Z., 2019. The effect of biochar amendment on N-cycling genes in soils: A meta-analysis. Sci Total Environ 696, 133984.
- [58] Yin, C., Yab, H., Cao, Y., Gao, H., 2023. Enhanced bioremediation performance of diesel-contaminated soil by immobilized composite fungi on rice husk biochar. Environ Res 226, 115663.
- [59] Yu, Q., He, J., Zhao, Q., Wang, X., Zhi, Y., Li, X., Li, X., Li, L., Ge, B., 2021. Regulation of nitrogen source for enhanced photobiological H_2 production by co-culture of *Chlamydomonas reinhardtii* and *Mesorhizobium sangaii*. Algal Res 58, 102422.
- [60] Zhang, B., Zhang, L., Zhang, X., 2019. Bioremediation of petroleum hydrocarbon-contaminated soil by petroleum-degrading bacteria immobilized on biochar. RSC 9 (60), 35304–35311.
- [61] Zhang, Z., Hou, Z., Yang, C., Ma, C., Tao, F., Xu, P., 2011. Degradation of n-alkanes and polycyclic aromatic hydrocarbons in petroleum by a newly isolated *Pseudomonas aeruginosa* DQ8. Bioresour Technol 102 (5), 4111–4116.
- [62] Zhang, S., Zhang, M., Han, F., Liu, Z., Zhao, C., Lei, J., Zhou, W., 2023. Enhanced degradation of petroleum in saline soil by nitrogen stimulation and halophilic emulsifying bacteria *Bacillus sp.* Z-13. J Hazard Mater 459, 132102.
- [63] Zhao, Y., Lu, Y., Zhuang, H., Shan, S., 2023. In-situ retention of nitrogen, phosphorus in agricultural drainage and soil nutrients by biochar at different temperatures and the effects on soil microbial response. Sci Total Environ 904, 166292.
- [64] Zheng, H., Liu, B., Liu, G., Cai, Z., Zhang, C., 2019. Chapter 19-Potential toxic compounds in biochar: knowledge gaps between biochar research and safety. Biochar Biomass- Waste 349–384.
- [65] Zhou, H., Jiang, L., Li, K., Chen, C., Lin, X., Zhang, C., Xie, Q., 2021. Enhanced bioremediation of diesel oil-contaminated seawater by a biochar-immobilized biosurfactant-producing bacteria *Vibrio sp.* LQ2 isolated from cold seep sediment. Sci Total Environ 793, 148529.
- [66] Zhou, H., Huang, X., Jiang, L., Shen, Q., Sun, H., Yi, M., Wang, X., Yao, X., Wu, Y., Zhang, C., Tang, J., 2023. Improved degradation of petroleum contaminants in hydraulic fracturing flowback and produced water using laccase immobilized on functionalized biochar. Environ Technol Innov 32, 103280.